Controlling of a Wind Turbine Driving Doubly-Fed Induction Generator using Adaptive Fuzzy-Self Tuning Controller

Ayman Safwat[1*], Mohiy E. Bahgat[1], A. M. Abdel-Ghany[2], Helmy M. El Zoghby[1]

[1]Electrical Power and Machines Department, Faculty of Engineering, Helwan University, Cairo, Egypt
[2]Electrical Power and Machines Department, Taiba Higher Engineering Institute, Cairo, Egypt
*ayman.safwat.pv6@gmail.com

Abstract. *Doubly fed induction generator is widely used in wind power extraction because of its higher efficiency and stability. For variable speed wind energy systems, the generator stator windings are directly connected to the grid. The generator rotor windings are connected to the grid through low rating back-to-back converter. In this work, vector control technique is used for obtaining decoupled control for active and reactive powers. In the other side. the employment of complex electronics makes controlling of doubly-fed induction generator (DFIG) is a big challenge because of its nonlinearity. Conventional controllers like proportional- integral (PI) controller do not give acceptable performance with uncertain dynamics, time delays, nonlinearity and change in the operating conditions. The design of traditional controller mainly based on the linear model of control systems. In this paper adaptive fuzzy self-tuning controller is proposed and designed for controlling the wind system at different operating conditions. Different simulation results are recorded using Matlab™/Simulink software. The simulation results are compared in case of using conventional PI controller and adaptive fuzzy self-tuning controller. The performance of the wind system is improved and has better performance in case of using adaptive fuzzy controller.*

1. Introduction

Wind energy is one of the renewable and popular energy sources. It is clean source and more penetration of it will reduce the use of fossil fuels that end and cause global warming. In addition, wind energy is everywhere and almost all the year time [1]–[3]. Cumulative wind energy worldwide reached 539 GW by the end of 2018 and is expected to exceed 760 GW by 2020 [4].Wind energy conversion system has different types which can be classified according to its operation into fixed speed and variable speed operation. The variable speed wind turbine can produce 8% to 15% more power compared to constant speed; however, they require electronic power converters to provide a constant frequency and constant voltage power for their loads [5]–[7].

Doubly fed induction generators (DFIGs) have seen a recent surge in popularity for wind turbine application for several reasons. The primaries reason for this their ability to vary their operating speed in order to gain optimum power extraction from the wind. This is achieved by feeding the rotor circuit with real and reactive power from the rotor side converter; the converter circuit allows the production or consumption of reactive power. In addition, for other variable speed generators, the DFIG power converter is rated low power (i.e. about 30% of the rated power of the wind turbine), as only a portion of the total energy supplied by the wind turbine is transferred through the converter. This makes wind turbines cheaper and lighter [8]–[11]. There are different control methods for controlling the rotor side converter of a DFIG [12]–[15]. The most common method is vector control; it can be used to perform decoupled control of generated active and reactive power. The direct rotor current i_{dr} is proportional to the stator reactive power and the quadrature rotor current i_{qr} is proportional to the torque or active stator power [16].

Conventional PI controllers are used to control the rotor side converter because of their simple structure and strong performance, its parameters are usually adjusted manually, using the MATLAB™ tuning option, or via conventional control methods [17], [18]. However, the main disadvantage of these fixed gain controllers is that their performance degrades due to changes in system operating conditions. Fuzzy logic controller (FLC) relies on human experience and considered as a heuristic approach to enhance the performance of the control system without the need of a detailed mathematical model. So, Fuzzy logic through a few years ago has recently emerged as a great tool in industrial applications [19], [20]. In recent years, fuzzy sets and fuzzy logic have been used to design fuzzy self-tuning of PI controller gains. The aim of the self-tuning PI controller design is to update the controller gains to meet a specific set of closed-loop system performance requirements [21].

In this work, a three-bladed horizontal-axis turbine based on a doubly fed induction generator (DFIG) is modeled. And thru this work, the aim to have a stable, fast and optimum control over the active and reactive power output of the generator is done by implementing a self-tuning fuzzy PI controller to manage the RSC using vector control and an indirect MPPT algorithm to maximize power extraction.

Fig .1 shows a schematic diagram of the DFIG connected to a wind turbine through a gearbox. The rotor of the DFIG is connected to a back-to-back converter. This converter has two parts: grid side converter (GSC) which is connected to the grid directly, and a rotor side converter (RSC) which is connected to the generator's rotor.

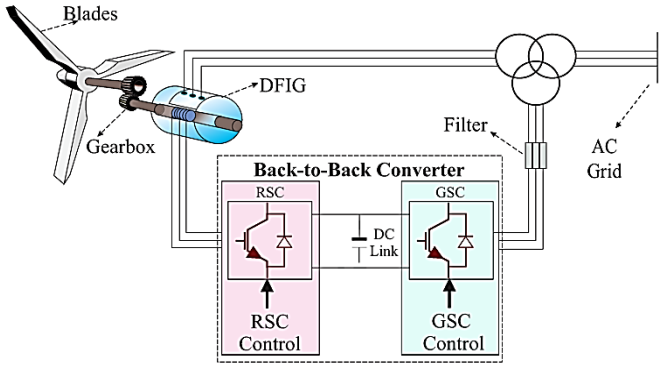

Fig. 1. Wind energy conversion system (WECS) using DFIG structure

2. THE PRPOSED SYSTEM MODEL

In this work, the DFIG model available in SimPowerSystem toolbox provided by MATLAB™/Simulink is used.

2.1. WIND TURBINE MODELING

The conversion of the wind power to mechanical power by the wind turbine rotor can be simulated by the static relation:

$$P_W = \frac{1}{2}\rho C_P(\beta, \lambda_i) A {V_W}^3 \quad (1)$$

Where P_w is the rotor mechanical power (W), V_w is the wind speed at the center of the rotor (m/s), A =πR^2 is the rotor surface (m^2), R is the rotor radius (m), ρ is the air density (kg/m^3), and CP is the rotor aerodynamic power coefficient [22]–[24].

$$C_P = K_1\left(\frac{K_2}{\lambda_i} - K_3\beta - K_4\beta^{K_5} - K_6\right)e^{\frac{K_7}{\lambda_i}} \quad (2)$$

$$\lambda_i = \frac{1}{\lambda + K_8} \quad (3)$$

Where λ is the tip speed ratio of the blade if the pitch angle of the blade (β) is constant and defined as:

$$\lambda = \frac{R\omega_R}{V_W} \quad (4)$$

Fig .2 shows the relation between the power coefficient and the tip speed ratio, it can be seen from the figure that the maximum power coefficient is 0.44 and the optimum tip speed ratio is 7.2

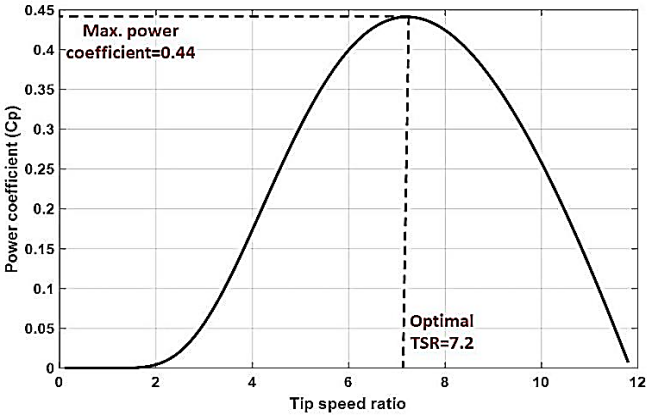

Fig. 2. C_P -λ performance curve for a modern three blade wind turbine

The rotor mechanical torque can be calculated from P_w by

$$T_W = \frac{P_W}{\omega_R} \quad (5)$$

Where ω_R is the rotor angular velocity in rad/sec. From (1) and (4), the rotor mechanical torque can be written as:

$$T_W = \frac{\rho C_P \pi R^2 {V_W}^3}{2\omega_R} = \frac{\rho C_P \pi R^3 {V_W}^2}{2\lambda} \quad (6)$$

$$C_t = \frac{C_P}{\lambda} \quad (7)$$

The rotor mechanical wind torque becomes

$$T_W = \frac{\rho \pi R^3 {V_W}^2}{2} C_t \quad (8)$$

Where C_t is the torque coefficient. This mechanical torque is used as input to the DFIG.

2.2. DOUBLY FED INDUCTION GENERATOR MODEL

Dynamic control of ac machine with three phase rotating phasor is somewhat complicated. Therefore, transformation (Park transformation) from three phases (ABC) to two phases (d-q) has been done by providing reference frame rotating at same speed of stator flux [25]–[27]. The dynamic equation for DFIG can be written in the d-q frame as

$$v_{ds} = R_s i_{ds} + \frac{d\psi_{ds}}{dt} - \omega_s \psi_{qs} \quad (9)$$

$$v_{qs} = R_s i_{qs} + \frac{d\psi_{qs}}{dt} + \omega_s \psi_{ds} \quad (10)$$

$$v_{dr} = R_r i_{dr} + \frac{d\psi_{dr}}{dt} - \omega_r \psi_{qr} \quad (11)$$

$$v_{qr} = R_r i_{qr} + \frac{d\psi_{qr}}{dt} + \omega_r \psi_{dr} \quad (12)$$

Developed electromagnetic torque can be written as

$$T_{em} = \frac{3}{2} P \frac{L_m}{L_S} (\psi_{qs} i_{dr} - \psi_{ds} i_{qr}) \quad (13)$$

Active and reactive power expression can be written as

$$P_S = \frac{3}{2} (v_{ds} i_{ds} + v_{qs} i_{qs}) \quad (14)$$

$$Q_S = \frac{3}{2} (v_{qs} i_{ds} - v_{ds} i_{qs}) \quad (15)$$

3. ROTOR SIDE CONVERTER CONTROL

Vector control strategy is implemented in Rotor Side Converter, where the d-axis of reference frame is aligned with the stator flux space vector [26]. Because of these choices developed electromagnetic torque and reactive power expression can be written as

$$T_{em} = -\frac{3}{2} P \frac{L_m}{L_S} |\overrightarrow{\psi_S}| i_{qr} \quad (16)$$

$$Q_S = -\frac{3}{2} \omega_S \frac{L_m}{L_S} |\overrightarrow{\psi_S}| (i_{dr} - \frac{|\overrightarrow{\psi_S}|}{L_m}) \quad (17)$$

This means that the q rotor current component controls the torque and, consequently, the speed of the machine. The d component rotor current controls the stator reactive power. Voltage equation in terms of rotor currents and stator flux can be written as

$$v_{dr} = R_r i_{dr} + \sigma L_r \frac{d}{dt} i_{dr} - \omega_r \sigma L_r i_{qr} \quad (18)$$

$$v_{qr} = R_r i_{qr} + \sigma L_r \frac{d}{dt} i_{qr} + \omega_r \sigma L_r i_{dr} + \omega_r \frac{L_m}{L_S} |\overrightarrow{\psi_S}| \quad (19)$$

Where: $\sigma = 1 - \frac{{L_m}^2}{L_S L_r}$

Reference d-q voltage equations are

$${v_{dr}}^* = U_{dr} - \omega_r \sigma L_r i_{qr} \quad (20)$$

$${v_{qr}}^* = U_{qr} + \omega_r \sigma L_r i_{dr} + \omega_r \frac{L_m}{L_S} |\overrightarrow{\psi_S}| \quad (21)$$

The control unit used in vector control is the traditional PI controller. The controller is designed according to the following formula [16]

$$U(t) = K_P e(t) + K_i \int e(t) dt \quad (22)$$

Where U (t) is controller output, e (t) is the error signal, K_P is proportional gain and K_i is integral gain.

Fig. 3 shows the rotor current control loops, where each current component is controlled by using a PI controller. The i_{dr} reference is usually set to zero. This is done to reduce the necessary rotor currents, thus reducing the dimensions of the rotor windings. This also allows limiting the control of reactive power generation exclusively on the GSC [26]. The i_{qr} reference is set according to indirect MPPT algorithm [28].

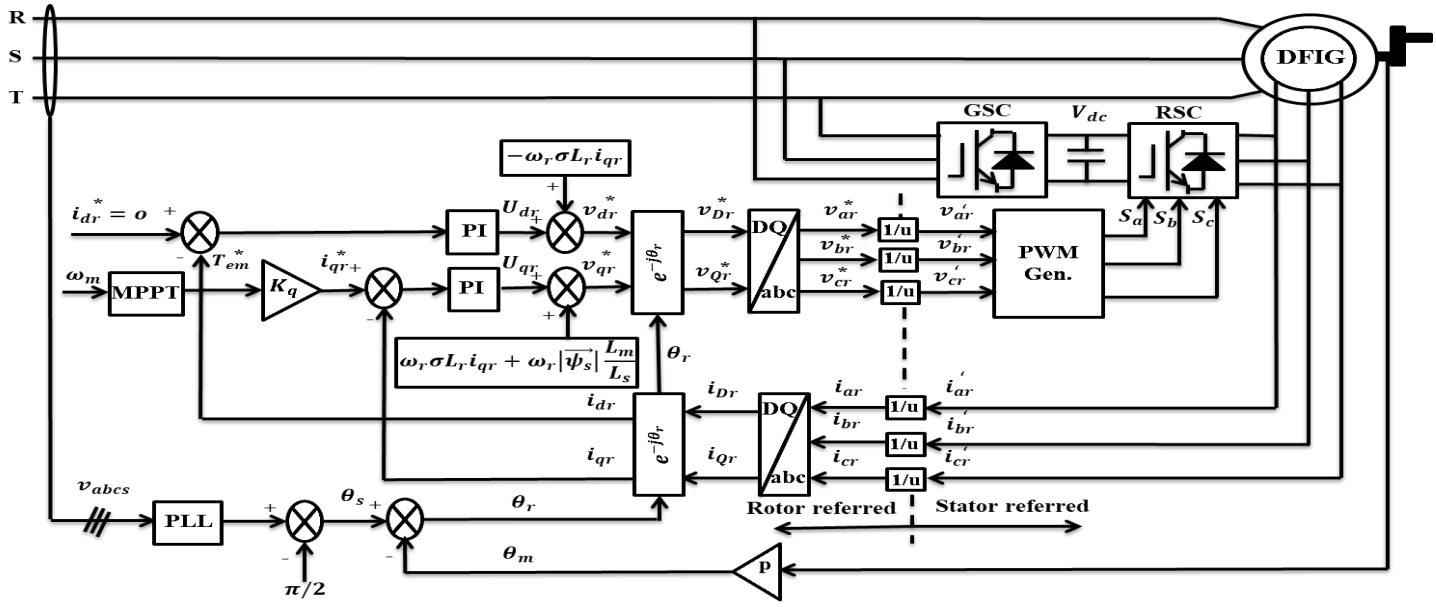

Fig. 3. Current control loops of the DFIG.

4. DESIGN OF A DAPTIVE FUZZY-SELF TUNING CONTROLLERS

There are many methods to tune controller parameters, the simplest is the Ziegler and Nichols method, but it is not guaranteed to be always effective. This paper looks into the self-tuning design of a PI controller. The controller has two parts: the conventional PI controller and the fuzzy logic control part, which has self-tuning capabilities. The proportional and integral gains (K_P, K_i) in a system can be automatically adjusted online as shown in Fig.4

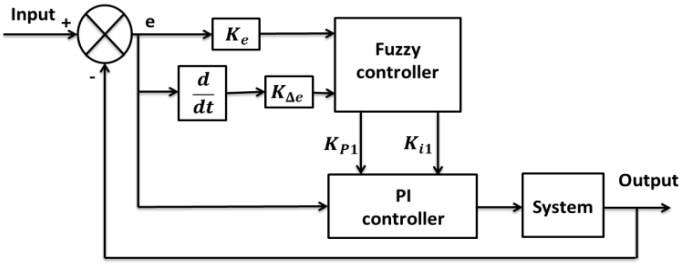

Fig. 4. Adaptive fuzzy-self tuning controller structure

The basic structure of the PI controller is described in the following formula

$$U(t) = K_P e(t) + K_i \int e(t)dt \quad (23)$$

After adding a fuzzy controller to adjust PI gains the equation becomes

$$U(t) = K_{P2} e(t) + K_{i2} \int e(t)dt \quad (24)$$

Where: $K_{P2} = K_P * K_{P1}$ and $K_{i2} = Ki * K_{i1}$
K_{P1}, K_{i1} are the gain outputs from fuzzy controller

The universe of discourse of error and change of error inputs to fuzzy must match its actual values either by taking the limits of the input periods as [e_{min} e_{max}] and [ce_{min} ce_{max}] or by placing normalization gains before entering the controller. Rule base and membership functions design are a matter of practice and expertise for the human operator, and there are no specific analytical steps to be implemented [29]. The linguistic labels of the inputs are {Negative Big, Negative medium, Negative Small, Zero, Positive small, Positive medium, Positive Big}, and in the rules bases are {NB, NM, NS, ZE, PS, PM, PB}.The linguistic labels of the outputs are {Zero, Medium small, Small, Medium, Big, Medium big, Very big}, and in rules bases are {Z, MS, S, M, B, MB, VB}.

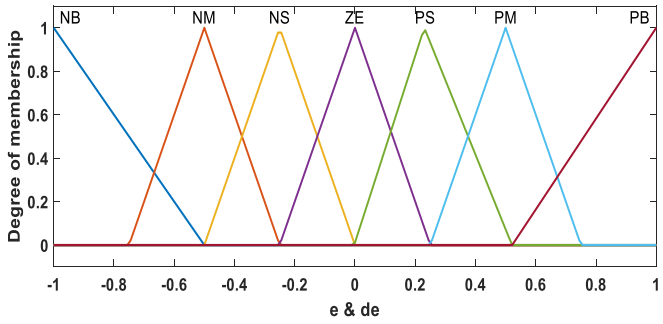

Fig. 5. Input membership functions of e and ce

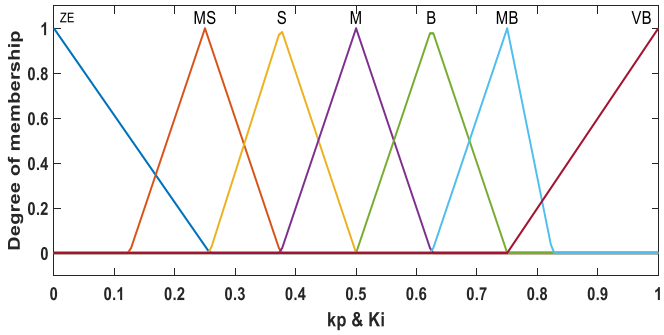

Fig. 6. Output membership functions

The values of K_e and $K_{\Delta e}$ are obtained by dividing the boundary values of the universe of discourse of the input member ship functions of e and Δe by the maximum actual values of e and Δe respectively, in order to normalize them within the limits of the member ship universe of discourse.

The rule base for determining K_{P1} and K_{i1} are shown in Tables .1 and 2 respectively.

Table 1. Rule base for determining K_{P1}

ce / e	NB	NM	NS	ZE	PS	PM	PB
NB	VB	VB	VB	VB	VB	VB	VB
NM	MB	MB	MB	MB	B	MB	VB
NS	B	B	B	B	MB	B	VB
ZE	ZE	ZE	ZE	MS	S	S	S
PS	B	B	B	B	MB	B	VB
PM	MB	MB	MB	MB	B	MB	VB
PB	VB	VB	VB	VB	VB	VB	VB

Table 2. Rule base for determining K_{i1}

ce / e	NB	NM	NS	ZE	PS	PM	PB
NB	M	M	M	M	M	M	M
NM	M	M	M	M	M	M	M
NS	S	S	S	S	S	S	S
ZE	MS	MS	MS	ZE	MS	MS	MS
PS	S	S	S	S	S	S	S
PM	M	M	M	M	M	M	M
PB	M	M	M	M	M	M	M

The last step is the defuzzification process that converts the fuzzy output to a crisp value for use as a non-fuzzy control action. The most popular method of defuzzification is the center of gravity or center of the area formulated as follows:

$$u = \frac{\sum_{i=1}^{r} u(u_i)u_i}{\sum_{i=1}^{r} u(u_i)} \quad (25)$$

Where $u(u_i)$is the membership grad (weight) of the element u_i which is the output of the rule i.

5. SIMULATION RESULTS AND ANALYSIS

The generator runs at a synchronous speed at t = 0 by setting the generator slip to 0 initially. A variable wind speed profile is used, which is simulated by summing multiple harmonics (Fig. 7) [30]–[32].

$$V_W = 8 + 0.4\sin(0.1047t) + 3.5\sin(0.2665t) + 0.4\sin(3.6645t) \quad (26)$$

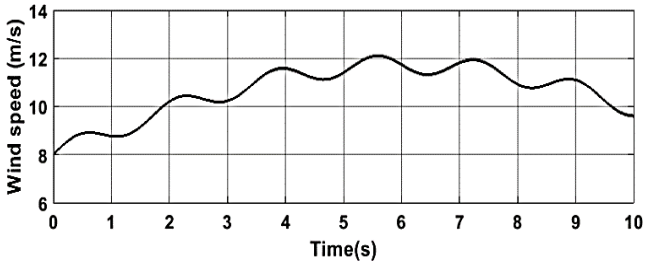

Fig. 7. Input wind speed profile

To evaluate the adaptive fuzzy PI performance, its results are compared to results obtained using a PI controller. The reason for this comparison is to monitor the effectiveness of the proposed controller versus the conventional controllers currently in use. Fig. 8 shows the rotor speed in rad/s, Fig. 9 illustrates the reference of the electromagnetic torque set by the MPPT algorithm for each controller, Fig. 10 shows i_{dr} current when using both a self-tuning fuzzy PI controller and a PI controller with the reference set to 0, Fig. 11 shows i_{qr} current, Fig. 12 shows the resulting electromagnetic torque and Fig. 13 shows the grid active power with both controllers.

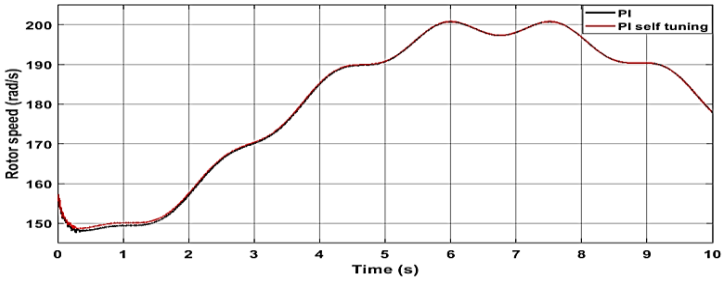

Fig. 8. Rotor speed using MPPT algorithm

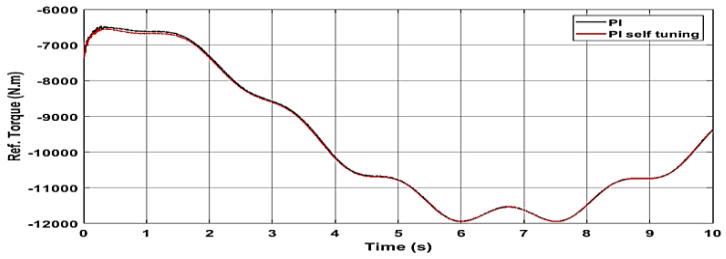

Fig. 9. Electromagnetic torque reference using MPPT.

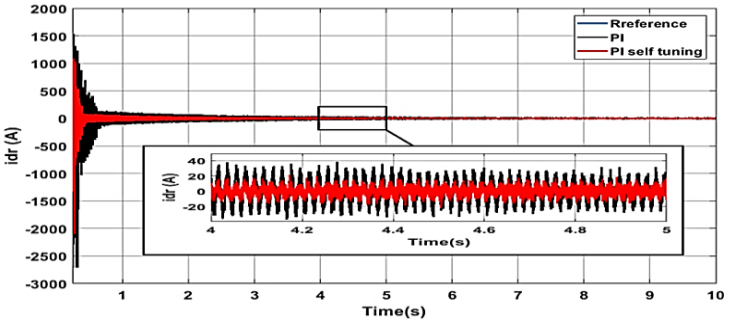

Fig. 10. i_{dr} current response

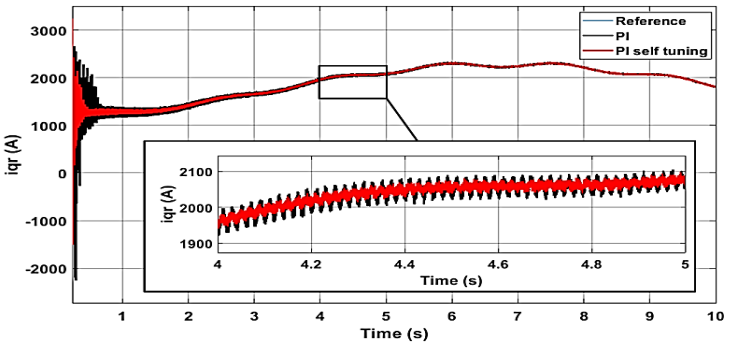

Fig. 11. I_{qr} current response

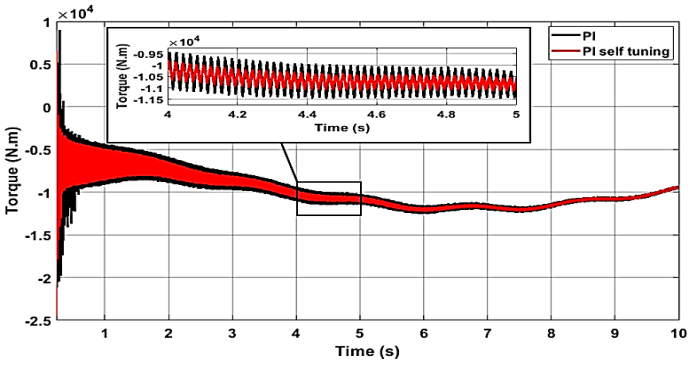

Fig. 12. Electromagnetic torque response

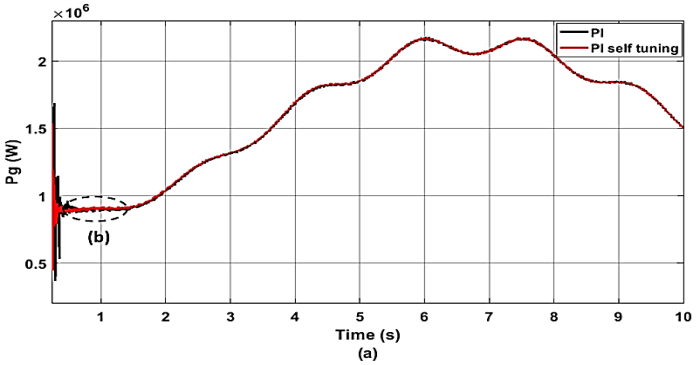

Fig. 13. (a) Grid active power

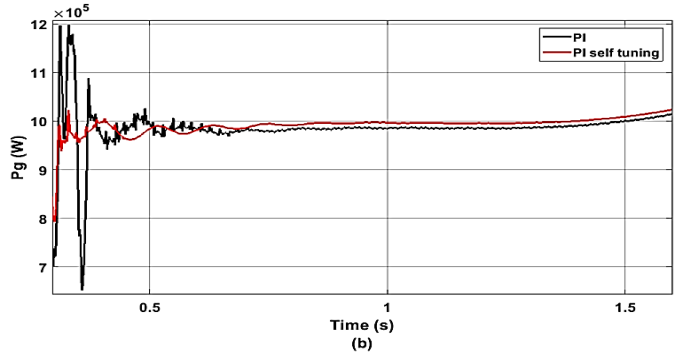

Fig. 13. (b) is zoomed section

6. Conclusions

This paper presented a comparison between the performances of a wind turbine driving DFIG using PI controller and adaptive fuzzy-self tuning PI controller. The two controllers are used for controlling the rotor side converter for a DFIG. A slight increase in the speed of the rotor is observed when using fuzzy self-tuning PI controller. This is due to the increased reference of the electromagnetic torque provided by the MPPT algorithm. So, the DFIG support more power. The rotor direct axis current is set to zero to limit the control of reactive power generation exclusively on the GSC. The system performance using adaptive fuzzy controller has smaller settling time, less fluctuations and more accurate response than conventional PI controller. Adaptive fuzzy controller is a robust and simple to design. In additions adaptive fuzzy controller doesn't require the knowledge of the exact model and it is efficiently used with linear and nonlinear systems.

Appendix

DFIG

Rated Stator power (Ps) = 2MW, Frequency (F) = 50 HZ, Synchronous speed = 1500 rpm, Pole pairs (p) = 2, Rated stator Voltage = 690V, Stator resistance (Rs) = 2.6mΩ, Rotor resistance (Rr) = 2.9mΩ, Stator / Rotor inductance (Ls/Lr) = 2.587mH.

Wind Turbine

Blade radius (R) = 42m, Nominal wind speed = 12.5 m/s, Gear ratio (N) = 100.

References

[1] K. Sun *et al.*, "VSC-MTDC system integrating offshore wind farms based optimal distribution method for financial improvement on wind producers," *IEEE Trans. Ind. Appl.*, vol. 55, no. 3, pp. 2232–2240, May 2019, doi: 10.1109/TIA.2019.2897672.

[2] A. Al-Dousari *et al.*, "Solar and wind energy: Challenges and solutions in desert regions," *Energy*, vol. 176, pp. 184–194, Jun. 2019, doi: 10.1016/j.energy.2019.03.180.

[3] D. M. Vijay, B. Singh, and G. Bhuvaneswari, "Position sensor-less synchronous reluctance generator based grid-tied wind energy conversion system with adaptive observer control," *IEEE Trans. Sustain. Energy*, vol. 11, no. 2, pp. 693–702, Apr. 2020, doi: 10.1109/TSTE.2019.2903891.

[4] S. Tao, Q. Xu, A. Feijoo, P. Hou, and G. Zheng, "Bi-Hierarchy Optimization of a Wind Farm Considering Environmental Impact," *IEEE Trans. Sustain. Energy*, vol. 11, no. 4, pp. 2515–2524, Oct. 2020, doi: 10.1109/TSTE.2020.2964793.

[5] R. Mittal, K. S. Sandhu, and D. K. Jain, "An Overview of Some Important Issues Related to Wind Energy Conversion System (WECS)," *Int. J. Environ. Sci. Dev.*, vol. 1, no. 4, pp. 351–363, 2010, doi: 10.7763/ijesd.2010.v1.69.

[6] X. Yin, W. Zhang, and X. Zhao, "Current status and future prospects of continuously variable speed wind turbines: A systematic review," *Mechanical Systems and Signal Processing*, vol. 120. Academic Press, pp. 326–340, Apr. 01, 2019, doi: 10.1016/j.ymssp.2018.05.063.

[7] D. K. Bhutto, J. Ahmed Ansari, S. S. Hussain Bukhari, and F. Akhtar Chachar, "Wind energy conversion systems (WECS) Generators: A review," Mar. 2019, doi: 10.1109/ICOMET.2019.8673429.

[8] S. Ghosh, Y. J. Isbeih, R. Bhattarai, M. S. El Moursi, E. F. El-Saadany, and S. Kamalasadan, "A Dynamic Coordination Control Architecture for Reactive Power Capability Enhancement of the DFIG-Based Wind Power

Generation," *IEEE Trans. Power Syst.*, vol. 35, no. 4, pp. 3051–3064, Jul. 2020, doi: 10.1109/TPWRS.2020.2968483.

[9] K. Liao, Z. He, Y. Xu, G. Chen, Z. Y. Dong, and K. P. Wong, "A Sliding Mode Based Damping Control of DFIG for Interarea Power Oscillations," *IEEE Trans. Sustain. Energy*, vol. 8, no. 1, pp. 258–267, Jan. 2017, doi: 10.1109/TSTE.2016.2597306.

[10] A. Dida, F. Merahi, and S. Mekhilef, "New grid synchronization and power control scheme of doubly-fed induction generator based wind turbine system using fuzzy logic control," *Comput. Electr. Eng.*, vol. 84, p. 106647, Jun. 2020, doi: 10.1016/j.compeleceng.2020.106647.

[11] M. Singh and S. Santoso, "Dynamic Models for Wind Turbines and Wind Power Plants," Golden, CO (United States), Oct. 2011. doi: 10.2172/1028524.

[12] S. Khateri-Abri, S. Tohidi, and N. Rostami, "Improved Direct Power Control of DFIG Wind Turbine by using a Fuzzy Logic Controller," in *2019 10th International Power Electronics, Drive Systems and Technologies Conference, PEDSTC 2019*, Apr. 2019, pp. 458–463, doi: 10.1109/PEDSTC.2019.8697581.

[13] Y. Sahri, S. Tamalouzt, and S. L. Belaid, "Direct Torque Control of DFIG Driven by Wind Turbine System Connected to the Grid," *2018 Int. Conf. Wind Energy Appl. Alger. ICWEAA 2018*, no. 2, pp. 1–6, 2019, doi: 10.1109/ICWEAA.2018.8605083.

[14] R. Nair and G. Narayanan, "Stator Flux Based Model Reference Adaptive Observers for Sensorless Vector Control and Direct Voltage Control of Doubly-Fed Induction Generator," in *IEEE Transactions on Industry Applications*, Jul. 2020, vol. 56, no. 4, pp. 3776–3789, doi: 10.1109/TIA.2020.2988426.

[15] H. Jenkal, B. Bossoufi, A. Boulezhar, A. Lilane, and S. Hariss, "Vector control of a doubly fed induction generator wind turbine," in *Materials Today: Proceedings*, Jan. 2019, vol. 30, pp. 976–980, doi: 10.1016/j.matpr.2020.04.360.

[16] A. R. Kumhar, "Vector Control Strategy to Control Active and Reactive Power of Doubly Fed Induction Generator Based Wind Energy Conversion System," *Proc. 2nd Int. Conf. Trends Electron. Informatics, ICOEI 2018*, no. Icoei, pp. 1–9, 2018, doi: 10.1109/ICOEI.2018.8553761.

[17] K. Ogata and Y. Yang, *Modern Control Engineering*. Upper Saddle River, NJ: Prentice hall, 2002.

[18] T. Hägglund, "The one-third rule for PI controller tuning," *Comput. Chem. Eng.*, vol. 127, pp. 25–30, Aug. 2019, doi: 10.1016/j.compchemeng.2019.03.027.

[19] E. Flores-Morán, W. Yánez-Pazmiño, and J. Barzola-Monteses, "Genetic algorithm and fuzzy self-tuning PID for DC motor position controllers," *Proc. 2018 19th Int. Carpathian Control Conf. ICCC 2018*, pp. 162–168, 2018, doi: 10.1109/CarpathianCC.2018.8399621.

[20] C. Conker and M. K. Baltacioglu, "Fuzzy self-adaptive PID control technique for driving HHO dry cell systems," *Int. J. Hydrogen Energy*, vol. 45, no. 49, pp. 26059–26069, Oct. 2020, doi: 10.1016/j.ijhydene.2020.01.136.

[21] H. Anantwar, D. B. R. Lakshmikantha, and S. Sundar, "Fuzzy self tuning PI controller based inverter control for voltage regulation in off-grid hybrid power system," in *Energy Procedia*, Jun. 2017, vol. 117, pp. 409–416, doi: 10.1016/j.egypro.2017.05.160.

[22] J. M. Nye, J. G. De La Bat, M. A. Khan, and P. Barendse, "Design and implementation of a variable speed wind turbine emulator," *Proc. - 2012 20th Int. Conf. Electr. Mach. ICEM 2012*, pp. 2060–2065, 2012, doi: 10.1109/ICElMach.2012.6350166.

[23] G. Abad, J. López, M. A. Rodríguez, L. Marroyo, and G. Iwanski, *Doubly Fed Induction Machine: Modeling and Control for Wind Energy Generation*. John Wiley & Sons, 2011.

[24] H. Ahuja and P. Kumar, "A novel approach for coordinated operation of variable speed wind energy conversion in smart grid applications," *Comput. Electr. Eng.*, vol. 77, pp. 72–87, Jul. 2019, doi: 10.1016/j.compeleceng.2019.05.004.

[25] B. Rached, M. Bensaid, M. Elharoussi, and E. Abdelmounim, "DSP in the loop Implementation of the Control of a DFIG Used in Wind Power System," *2020 1st Int. Conf. Innov. Res. Appl. Sci. Eng. Technol. IRASET 2020*, no. 6, 2020, doi: 10.1109/IRASET48871.2020.9092165.

[26] H. Abu-Rub, M. Malinowski, and K. Al-Haddad, *Power Electronics for Renewable Energy Systems, Transportation and Industrial Applications*, vol. 9781118634. John Wiley & Sons, 2014.

[27] F. M. Gebru, B. Khan, and H. H. Alhelou, "Analyzing low voltage ride through capability of doubly fed induction generator based wind turbine," *Comput. Electr. Eng.*, vol. 86, p. 106727, Sep. 2020, doi: 10.1016/j.compeleceng.2020.106727.

[28] D. Song, J. Yang, M. Su, A. Liu, Y. Liu, and Y. H. Joo, "A comparison study between two MPPT control methods for a large variable-speed wind turbine under different wind speed characteristics," *Energies*, vol. 10, no. 5, 2017, doi: 10.3390/en10050613.

[29] H. X. Li and S. K. Tso, "Quantitative design and analysis of fuzzy proportional-integralderivative control a step towards autotuning," *Int. J. Syst. Sci.*, vol. 31, no. 5, pp. 545–553, Jan. 2000, doi: 10.1080/002077200290867.

[30] and H. B. F. Kendouli, K. Nabti, K. Abed, "Modélisation, simulation et contrôle d'une turbine éolienne à vitesse variable basée sur la génératrice asynchrone à double alimentation," *Rev. des Energies Renouvelables*, vol. 14, no. 1, pp. 109–120, 2011.

[31] O. A. M. Ali, H. M. El-Zoghby, and A. G. M. A. Ghany, "Maximizing the Generated Power from Hybrid Wind-Solar System Based on Fuzzy Self Tuning Single Neuron PID Controller," *2018 20th Int. Middle East Power Syst. Conf. MEPCON 2018 - Proc.*, pp. 748–753, 2019, doi: 10.1109/MEPCON.2018.8635230.

[32] H. M. Abdel, M. Sayed, S. M. Sharaf, S. E. Elmasry, and M. Elharony, "Simulation of the Different Transmission Line Faults for a Grid Connected Wind Farm with Different Types of Generators," *Int. J. Power Electron. Drive Syst.*, vol. 1, no. 2, pp. 179–189, 2011.